

Structure and conformational properties of ideal nanogel particles in athermal solutions

Alexandros Chremos,^{1, a)} Ferenc Horkay,^{1, b)} and Jack F. Douglas^{2, c)}

¹⁾*Section on Quantitative Imaging and Tissue Sciences, Eunice Kennedy Shriver National Institute of Child Health and Human Development, National Institutes of Health, Bethesda, MD 20892, USA*

²⁾*Materials Science and Engineering Division, National Institute of Standards and Technology, Gaithersburg, Maryland 20899, USA*

(Dated: 14 September 2021)

We investigate the conformational properties of ‘ideal’ nanogel particles having a lattice network topology by molecular dynamics simulations to quantify the influence of polymer topology on the solution properties of this type of branched molecular architecture. In particular, we calculate the mass scaling of the radius of gyration (R_g) and the hydrodynamic radius, as well as, the intrinsic viscosity with the variation of the degree of branching, the length of the chains between the branched points, and the average mesh size within these nanogel particles under good solvent conditions. We find competing trends between the molecular characteristics, where an increase in mesh size or degree of branching results in the emergence of particle-like characteristics, while an increase in the chain length enhances the linear polymer-like characteristics. This crossover between these limiting behaviors is also apparent in our calculation of the form factor, $P(q)$, for these structures. Specifically, a primary scattering peak emerges, characterizing the overall nanogel particle size. Moreover, a distinct power-law regime emerges in $P(q)$ at length scales larger than the chain size, but smaller than the R_g of the nanogel particle, and the R_g mass scaling exponent progressively approaches zero as the mesh size increases, the same scaling as for an infinite network of Gaussian chains. The ‘fuzzy sphere’ model does not capture this feature, and we propose an extension to this popular model. These structural features become more pronounced for values of molecular parameters that enhance the localization of the branching segments within the nanogel particle.

I. INTRODUCTION

The versatile role of gels as a building block in a wide variety of biological^{1,2} and chemical systems, such as scaffolds for tissue engineering,^{3–5} medical applications⁶ and personal care products^{7,8} has attracted considerable attention in the last decades. The unique physical properties of gels that make them attractive in applications ultimately arise from their structure, i.e., a crosslinked polymer network immersed in a solvent.^{9,10} While such materials have been the subject of experimental and theoretical investigations for more than half a century, their rational design and characterization remains challenging. This is particularly true for nanogel particles because the size of the polymer network becomes comparable to the size of the polymer chains which compose it. One example where nanogel particles have become indispensable is drug delivery,^{11–13} where a hydrophobic drug is often formulated together with a small network of polymer chains (nanogel particle) into an amorphous solid dispersion. The use of nanogel particles as a drug delivery vehicle needs to satisfy the following conditions: (i) tunable particle size for the enhanced permeability and retention effect; (ii) carrier and encapsulation stability to prevent premature drug release

before approaching the target site; (iii) payload release should be triggered by external stimuli in the target cell environment. All these applications are highly dependent on the structure of nanogel particles, which can be tuned through variation of the polymer network topology. Understanding how these structural characteristics influence nanogel particles’ configurational properties should aid in designing nanogel particles for the desired application.

One of the main challenges in the design of macrogels and nanogel particles is that often there is little understanding of how the microscopic structure of such materials impacts the (nano)gel’s properties.^{14–18} Direct knowledge of the (nano)gel structure mostly originates from scattering (neutron or x-rays) experiments,^{19–22} but the conclusions remain qualitative since there is a degeneracy of different types of structure that may exhibit similar scattering form factors $P(q)$. The classical model of infinite ideal networks of Gaussian chains is well known, however, it is also generally appreciated that the neglect of excluded volume interactions in this model to property predictions differs from real macroscopic networks.^{23–29} The modeling of gels by computer simulation can provide a unique window in microscopic structure of gels over a wide range of gel molecular topologies and evaluate different theoretical models.^{15–18,30,31} Primary focus in the development of these computational models has been on the nature of swelling in these branched polymers. However, there are two main limitations of the existing computer models of (nano)gels. First, a *phenomenological* methodology

^{a)}Electronic mail: alexandros.chremos@nih.gov

^{b)}Electronic mail: horkayf@mail.nih.gov

^{c)}Electronic mail: jack.douglas@nist.gov

is often utilized to mimic the synthesis of a specific gel system bounded by the assumptions and observations of experimentalists. Second, most studies that utilize such models confine over a narrow set of molecular parameters due to immense parameter space that define the gel structure. While these models have provided significant insights, the original challenge of establishing *general* guidelines in the optimum design of nanogel particles remains unresolved.

In our study, we develop a general nanogel particle model to gauge the contribution of different molecular parameters on its conformational properties, thus avoiding potential nuances originating by mimicking the random processes of assembly occurring in the course of synthesis. Specifically, we focus on nanogel particles that have the following features: regular (the elementary building block is the same throughout the nanogel structure), compactness (the nanogel is dominated by the formation of loops), and perfect topological regularity of structure, i.e., there are no ‘defects’. Previous studies of (nano)gels with these features have primarily utilized the lattice-like connectivity to study the network elasticity and phase transitions in these structures.³¹ For the purposes of our study, we focus on the star polymer arranged on a cubic lattice. The reason behind these choices is threefold: (a) the structures in our study can be used as reference points since these structures do not depend on phenomenological random processes and thus there is less ambiguity in the character of these structures, (b) there is an increased interest in the synthesis of ‘ideal networks’ as bulk gel materials,^{32–35} and (c) as part of future work we will study the effects of ‘defects’ in the nanogel structure by utilizing the nanogel model of our current study as a reference model.

The present paper focuses on the conformational properties of ‘ideal’ nanogel particles, which can be viewed as branched polymers having a compact structure. In particular, we calculate mass scaling of the radius of gyration and the hydrodynamic radius, as well as, the intrinsic viscosity over a wide range of molecular masses and molecular architectures. To better understand the structure of these nanogel particles, we also calculate the form factor and compare our results with the ‘fuzzy sphere’ model,³⁶ we also propose an extension to improve the description of the form factor for the internal structure of nanogel particles. Our results provide insights into the nature of nanogel particles and their conformational properties, and we identify conditions for the emergence of gel-like characteristics.

The paper is organized as follows. Section II contains details of the coarse-grained nanogel particle model and the simulation methods. The results are presented in section III, where we investigate the influence of topology on the conformational properties of the nanogel particles in subsection III A, the scattering profiles that these structures exhibit in subsection III B, comparison with the ‘fuzzy sphere’ model in subsection III C, and a brief comparison with perfect gels is in subsection III D.

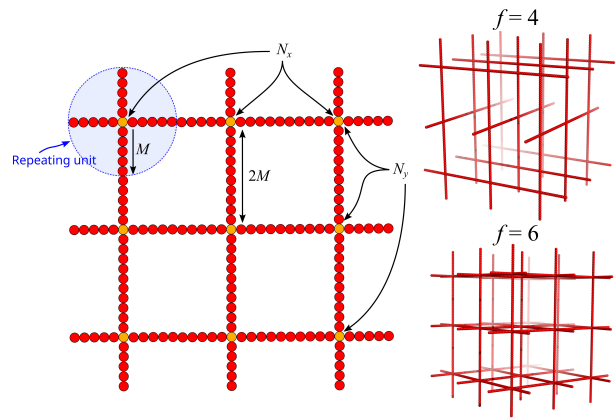


FIG. 1. Schematic of the molecular architecture of the nanogel particle, along with two screenshots of the initial configuration of two nanogel particles having different degrees of branching, f , and a mesh size of $N_b = 3$.

Finally, we draw our conclusions in Sec. IV.

II. METHODS AND MODELS

A. Model and molecular dynamics

We employ a bead-spring model suspended in an implicit solvent. All particles are assigned the same mass m , size σ , and strength of interaction ε ; we set ε and σ as the units of energy and length. The segmental interactions are described by the cut-and-shifted Lennard-Jones (LJ) potential with a cutoff distance $r_c = 2^{1/6} \sigma$, corresponding to an athermal solvent. The segments along a chain are connected with their neighbors via a stiff harmonic spring, $V_H(r) = k(r - l_0)^2$, where $l_0 = 0.99 \sigma$ is the equilibrium length of the spring, and $k = 2500 \varepsilon / \sigma^2$ is the spring constant.

The repeating structural unit of the polymer network studied here is a branched structure having the form of a regular star polymer. A regular star polymer has a core particle, which is connected with the free end of f chains (or arms) composed of M segments. Thus, the total number of interaction centers per star polymer is $M_{w,\text{star}} = fM + 1$. A regular polymer network is composed by star polymers placed in a cubic lattice and with two or more of their free ends bonded with the free ends of the neighboring stars, the number of branched points (or star polymers) in each direction are labelled as N_x , N_y , and N_z , see Fig. 1. The molecular mass of a nanogel particle is $M_w = (N_x N_y N_z) M_{w,\text{star}}$. We use the quantity N_b to characterize the size of the mesh as a whole, since we focus on nanogel particles having $N_b = N_x = N_y = N_z$. We note that by ‘mesh size’ is typically referred in the literature to the average size of the compartment created by the polymer chains that form the mesh. For the purposes of our current study, we instead refer to ‘mesh size’ as the size of the whole

mesh. We note that every star polymer unit at the interior of the nanogel is fully bonded with its neighbors and thus the only dangling polymer chains are located at the exterior of the nanogel structure. This type of nanogel particles is dominated by both branches and loops. We also note that nanogels particles having $f = 4$ result in the formation of fewer but larger loops compared to $f = 6$ nanogel particles, see Fig. 1.

The systems were equilibrated at constant temperature $k_B T/\varepsilon = 1.0$ conditions, maintained by a Nosé-Hoover thermostat. Typical simulations equilibrate for 5000τ and data is accumulated over a 150000τ interval, where $\tau = \sigma(m/\varepsilon)^{1/2}$ is the MD time unit; the time step used was $\Delta t/\tau = 0.005$.

B. Path-integration package, ZENO

Hydrodynamic radius and intrinsic viscosity calculations are based on the use of path-integration algorithm ZENO, which calculates hydrodynamic, electrical, and shape properties of polymer and particle suspensions,³⁷⁻³⁹ and has been used in many real systems.^{40,41} The computational method used by ZENO for calculating R_h , as well other hydrodynamic properties, involves placing a polymeric structure inside an enclosing sphere and then launching random walks from the surface of the sphere. The fraction of walks that hit the molecule as opposed to walks ending in infinity can be directly related to R_h . We repeat this process for 10^4 distinct molecular conformations and then construct distributions of R_h for each molecular topology and M_w . We also determine the mean and the standard deviation for these distributions. Through an extension of the process just described,³⁸ which considers both where the launched trajectories initiate on the probing sphere and where they end when they hit the polymer, other basic polymer characterization properties can be estimated from ZENO such as the intrinsic conductivity of conducting particles and the intrinsic viscosity due to the mathematical similarities between electrical and hydrodynamical properties.^{38,42}

III. RESULTS AND DISCUSSION

We first obtain the mass scaling behavior of the average radius of gyration (R_g), hydrodynamic radius (R_h), and intrinsic viscosity ($[\eta]$) of nanogel particles in athermal solvent with the variation of size of the overall mesh structure, chain length, and degree of branching. Following this analysis, we make comparisons between nanogel particles and linear chains. Subsequently, we calculate the form factor for these structures and identify the conditions at which particle-like features start to emerge in the scattering profiles. We also compare the ‘fuzzy sphere’ model and propose an extension to improve the description of the form factor of nanogel particles’ internal structure.

A. Conformational properties of nanogel particles

Before we discuss the findings of our computational investigation of ideal nanogel particles, we briefly revisit the scaling of their average size in solution (e.g., radius of gyration, R_g) with increasing molecular mass M_w of basic classes of polymers: Linear and random branched polymers. In particular, R_g scales as M_w^ν in athermal solvents with $\nu \approx 10/17 \approx 0.588$ and $\nu = 1/2$ for self-avoiding walks and lattice animals in three dimensions, respectively,⁴³⁻⁴⁶ and near the θ -point in solution at which attractive interactions between the polymer segments compensate the repulsive binary excluded volume interactions we have $\nu = 1/2$ for linear chains⁴⁷ and $\nu \approx 2/5$ for randomly branched polymers in the high mass limit.⁴⁸⁻⁵⁰ A basic feature of randomly branched polymers in good (athermal) solvents (‘lattice animals’) is that the number of branching points tends to grow linearly with the polymer mass so that such polymers can be thought of as imperfect sheet-like polymers, i.e., having a topological dimensionality of two.⁵⁰ Polymers having different topologies than linear chains and randomly branched polymers raise the question of how their scaling characteristics relate to polymers having a different topological structure.

We first investigate nanogel particles without altering their topology by keeping *fixed* size of the mesh as a whole, N_b , and the degree of branching, f . The length of the chains connecting the branching points, M , is the only parameter that we vary. The resulting average radius of gyration, R_g , was found to scale as $R_g \sim M_w^{0.588 \pm 0.03}$ for all the molecular masses and values of f of nanogel particles explored in our study, see Fig. 2a. This is understandable since the scaling exponent is the same as the known value for self-avoiding random walks. The degree of branching for nanogel particles having $M = 15$ is still important since it influences the prefactor of the scaling relation, i.e., $R_g(f = 4)/R_g(f = 6) \approx 1.22$ of equivalent M_w for $M = 15$. For the hydrodynamic radius, R_h , we find a mass scaling exponent of $R_h \sim M_w^{0.63}$. The ratio R_h/R_g is often used to characterize the molecular shape of an object, where $R_h/R_g \approx 1.28$ for a perfect sphere, $R_h/R_g \approx 0.8$ for random walk, and $R_h/R_g \rightarrow 0$ for infinite long rod. The molecular shape of the nanogel particles having fixed N_b and f is found $R_h/R_g \approx 1.18$ for $f = 4$ and $R_h/R_g \approx 1.22$ for $f = 6$, implying that the overall molecular shape of these nanogel particles is rather compact, and thus it is not influenced by M variation.

Next, we focus on the mass scaling of the nanogel particles having f and M fixed, but with increasing N_b . Overall, we find R_g to scale as $R_g \sim M_w^{1/3}$ through the whole M_w range, see Fig. 3a. We note that a deviation is observed for $N_b = 1$, which is reasonable since the structure becomes then a star polymer instead of a polymer network. This scaling exponent found as the mesh size increases indicates the emergence of particle-like charac-

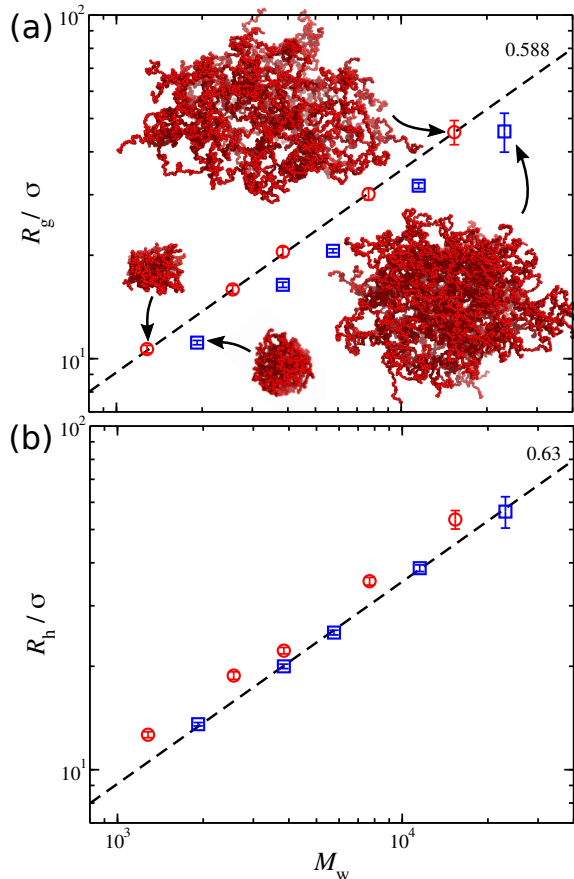


FIG. 2. (a) Radius of gyration, R_g , and (b) hydrodynamic radius, R_h , of regular polymer networks with number of branches $f = 4$ (circles) and $f = 6$ (squares) as a function of molecular mass, M_w . All nanogel particles have the same mesh size, $N_b = 4$, and so M_w increases by increasing the chain length M . The uncertainty estimates correspond to two standard deviations.

teristics. The effect of f in the R_g mass scaling appears to be small in the example presented in Fig. 3a, but we will discuss this in more detail below. Near identical behavior is found in our calculations for R_h , Fig. 3b.

The R_g mass scaling exponent of the nanogel particle depends on the manner in which M_w is increased. On the one hand, we observe the emergence of particle-like characteristics $\nu \approx 1/3$ as the mesh size increases, while, on the other hand, we find polymer-like characteristics $\nu \approx 0.588$ as the nanogel topology remains invariant and M increases. This duality in the mass scaling exponent reflects the dual nature of nanogel particles, where their properties range from a (soft) particle to polymer-like characteristics.

To better understand this behavior of R_g , we compare them to the average radius of gyration of a linear chain, $R_{g,\text{linear}}$. A branched polymer structure, such as a star polymer or a bottlebrush polymer, is more compact than a linear chain.^{48,51,52} Thus, we expect a nanogel particle, whose properties are greatly influenced by its

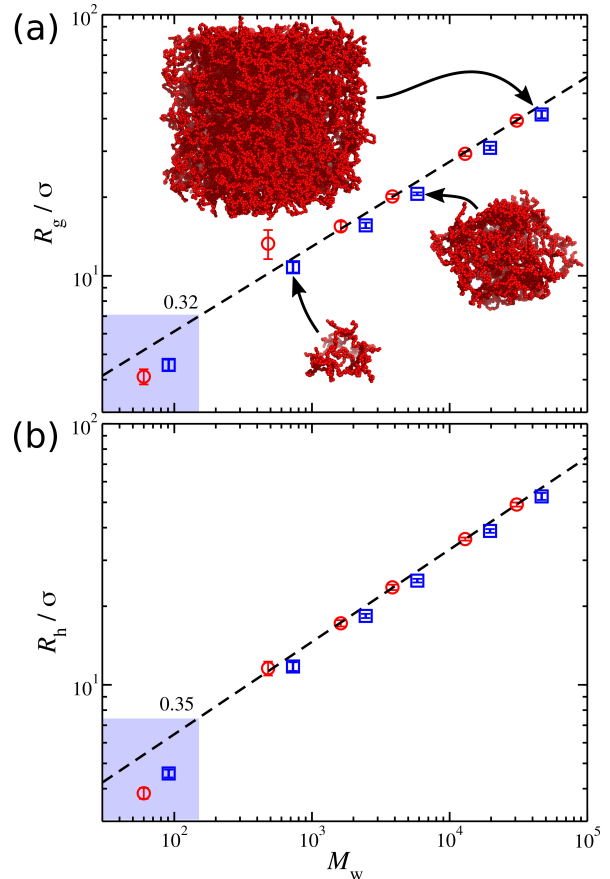


FIG. 3. (a) Radius of gyration, R_g , and (b) hydrodynamic radius, R_h , of regular polymer networks having $M = 15$ and number of branches $f = 4$ (circles) and $f = 6$ (squares) as a function of molecular mass, M_w , by increasing the size of the mesh as a whole, N_b . The highlighted regions outline structures that do not contain loop structures, i.e., $N_b = 1$, corresponding to regular star polymers. The uncertainty estimates correspond to two standard deviations.

branches and loops, to exhibit a high degree of compactness compared to a linear chain. One possible approach to describe in quantitative terms this effect was introduced by Zimm and Stockmayer^{53,54} by defining a geometric shrinking factor as the ratio of the average radius of gyration of the polymer structure of interest over the average radius of gyration of linear chain, $R_g/R_{g,\text{linear}}$, of the same M_w . As expected, we find that an increase in the mesh size results in a significant decrease in $R_g/R_{g,\text{linear}}$, see Fig. 4. The rate of this decrease is found to follow a power-law $R_g/R_{g,\text{linear}} \sim (1/M_w)^\alpha$, where $\alpha = 0.26$ for $f = 6$ and $\alpha = 0.23$ for $f = 4$. Interestingly, the degree of branching results in a decrease of $R_g/R_{g,\text{linear}}$ in nanogel particles having small mesh size, $N_b \lesssim 5$, where the nanogel particle resembles more a regularly branched polymer (star, comb, knotted ring) than a polymer network. Indeed, $R_g/R_{g,\text{linear}}$ for $N_b = 2$ and $f = 4$ nanogel particles exhibit approximately the same degree of compactness as with that

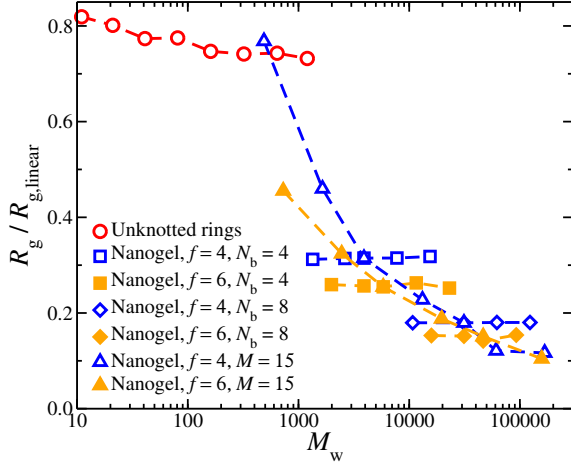


FIG. 4. Ratio of average radius of gyration of nanogel particle over the average radius of gyration of a linear chain, $R_g/R_{g,\text{linear}}$, with the same molecular mass, M_w . Results of unknotted ring polymers are also presented.

of unknotted ring polymers, which is a polymer structure of a single loop without any branches. This decrease in $R_g/R_{g,\text{linear}}$ becomes smaller as the mesh size increases and for $N_b \gtrsim 10$ the difference becomes negligible (Fig. 4), suggesting that at this point, the nanogel particle becomes rather compact and can be effectively described by Gaussian statistics. An increase of M does not influence $R_g/R_{g,\text{linear}}$, which is consistent with our findings above.

The size and compactness of nanogel particles also influence the hydrodynamic solution properties. The viscosity of a dilute dispersion of particles can be developed in a power series in the particle volume fraction (ϕ) as,

$$\eta(\text{dispersion}) = \eta(\text{dispersing fluid})\{1 + [\eta]\phi + O(\phi^2)\}. \quad (1)$$

The first coefficient in ϕ is independent of interparticle interaction and is conventionally called the ‘‘intrinsic viscosity’’, $[\eta]$, and is defined in the limit of the particle concentration in the solution $c \rightarrow 0$ as,

$$[\eta] = \lim_{c \rightarrow 0} \frac{\eta - \eta_s}{c \eta_s}, \quad (2)$$

where η and η_s are the solution and solvent viscosity. The intrinsic viscosity is a useful metric to characterize how a molecular structure influences the hydrodynamic properties of the solution, especially in the dilute regime^{55–57} and solution properties are often described in reduced concentration, e.g., $c[\eta]$. For the purposes of the current study, we use the path-integration algorithm ZENO, which calculates hydrodynamic, electrical, and shape properties of the polymer and particle suspensions, as described in the subsection II B. In practice, the molecular mass dependence of the intrinsic viscosity is represented by the Mark-Houwink equation, $[\eta] = KM_w^\alpha$,^{43,58,59} where K and α are material-

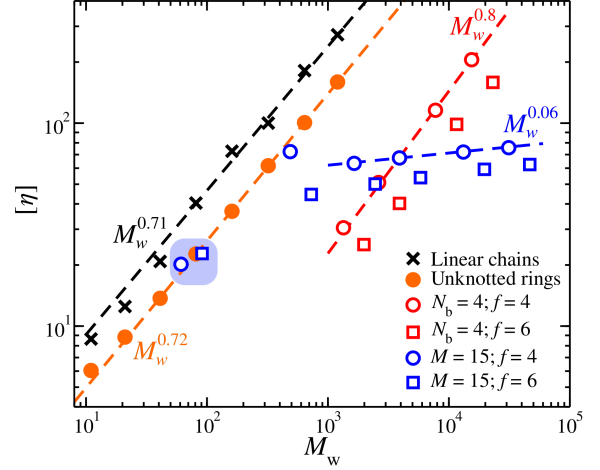


FIG. 5. Intrinsic viscosity, $[\eta]$, of ideal nanogel particles as a function of the molecular mass, M_w . Results for linear chains and unknotted ring polymers are also presented. The dashed lines are power-laws as guides for the eye. The light blue highlighted region outlines nanogel particles having a mesh size of $N_b = 1$, corresponding to star polymers.

specific parameters. The exponent α becomes $\alpha \approx 0.71$ and $\alpha \approx 0.5$ for linear polymer chains in good and θ -solvent conditions, respectively. This is supported by experimental^{60,61} and simulation studies,⁶² as well as the calculations in the current study, see Fig. 5. However, deviation from this is expected for molecular structures that differ from linear polymer chains. For example, $\alpha \approx 2$ for perfectly rod-like polymers like Tobacco mosaic virus,⁶³ and typical values of α for rather stiff polymers are typically somewhat larger than 1. ‘Semi-flexible’ polymers exhibit α values close but greater than 0.8.⁶⁴

Nanogel particles exhibit significantly smaller $[\eta]$ than the corresponding value for linear chains at the same M_w , providing a measure of their compact nature. We also find that the mass scaling exponent α exhibits different values depending on how the molecular mass of the nanogel increases. We find $\alpha \approx 0.8$ by increasing M , Fig. 5. This suggests that the nanogel particles increase the viscosity of the solution as a function of M_w in a fashion similar to polymers with some intrinsic stiffness, although linear polymer chains tend to have a larger overall molecular size, see Fig. 4. A possible explanation is that an increase of M in conjunction with the mesh structure of the nanogel particle influence the spatial distribution of the nanogel’s segments in a way that would more efficiently alter the dynamic properties of the solution. However, we find that α becomes relatively small for nanogel particles having M fixed where N_b is increasing, Fig. 5. We had not initially expected this trend, which accords with the mass scaling of the size of an perfect infinite network of Gaussian chains, i.e., no excluded volume interactions.²⁷ In particular, the size of such networks depends only on average size of an indi-

vidual chain within the network even if there are infinite number of such links in the network. This same trend is reflected in the equilibrium size of the nanogel particles, see Fig. 5. For comparison, $[\eta] = 5/2$ for rigid spheres at infinite dilution,⁶⁵ where $[\eta]$ is constant irrespective of the molecular mass of the spheres, and $[\eta]$ takes a slightly larger values for cube-like objects, e.g., for rigid cubes with sharp edges $[\eta] \approx 3.04$.^{57,66} This observation suggests that the nanogel particles with increasing their mesh size behave similarly to rigid spheres and cubes. Interestingly, comb polymers having long side chains, i.e., 'bottlebrush polymers', have also been observed to exhibit vanishing small α values,⁶⁰ suggesting that branched polymers that form densely filled, non-draining, rigid sphere-like conformation, exhibit vanishing small α values.

We note that when $N_b < 3$ the structure of the nanogel particle resembles more a swollen randomly branched polymer, i.e., lattice animal. Thus, it is no surprise that $[\eta]$ values become comparable to $[\eta]$ values of linear polymer chains and unknotted ring polymers. Overall, these trends suggest that an increase in M will significantly increase the viscosity of the solution while an increase in N_b will not significantly influence it. An increase in the degree of branching suppresses $[\eta]$, but does not influence the mass scaling exponent. These simple design rules should be useful in applications.

B. Nanogel Form Factor

To probe the structure of nanogel particles, we focus on calculating the spatial correlations between the polymer segments. The form structure factor, $P(q)$, is a suitable property for this purpose and describes the mean correlations in the positions of a collection of point particles distributed in space. $P(q)$ is defined as:

$$P(q) = \frac{1}{M_w} \left\langle \sum_{j=1}^{M_w} \sum_{k=1}^{M_w} \exp[-i\mathbf{q} \cdot (\mathbf{r}_j - \mathbf{r}_k)] \right\rangle, \quad (3)$$

where $i = \sqrt{-1}$, $q = |\mathbf{q}|$ is the wave number, \mathbf{r}_j is the position of particle j , $\langle \rangle$ denote the time average.

We start with some general comments on the calculation of $P(q)$ and about the common scattering features of these systems. At small q -values corresponding to length scales much larger than the size of a nanogel or a polymer structure, $q\sigma < 2\pi/R_g$, $P(q)$ rapidly increases and reaches a plateau $P(q) \approx M_w$. At high q -values, a scattering peak is anticipated at $q\sigma \approx 7$ corresponding to the segment-segment distance (not shown here). At length scales larger than segment size but smaller than the size of the polymer chains composing the nanogel particles, i.e., $\pi/M < q\sigma < 7$, a power-law behavior is expected that will describe the conformation of these polymer chains. The behavior of $P(q)$ in length scales larger than the polymer chains but smaller than the nanogel particle will provide information on the molec-

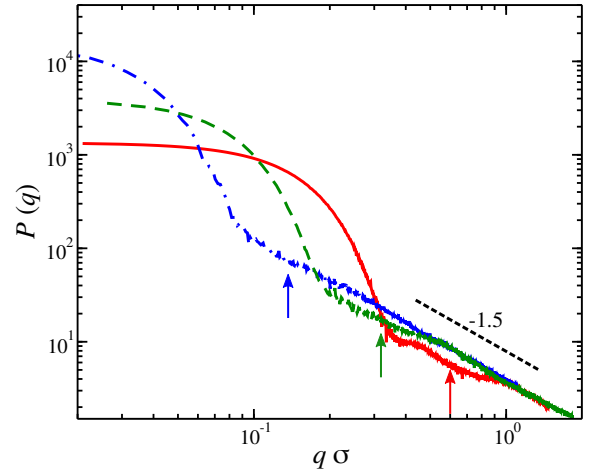


FIG. 6. The form factor $P(q)$ of ideal nanogel particles having $N_b = 4$ and $f = 4$ at different values of M : continuous line $M = 5$, dashed line $M = 15$, and dot-dashed line $M = 60$. The arrows indicate the average R_g of the nanogel particles.

ular topology of these particles. In other words, it provides information about the nature of the chain network, which is the central focus of the current study.

The scattering profiles of nanogel particles with a small mesh size, $N_b \lesssim 5$ at different values of M variation exhibits a power-law scaling of $q^{-1.6}$ for $q\sigma > 2\pi/R_g$. This power-law scaling behavior indicates that the polymer chains composing the nanogel structure adopt conformations that lie between a rod ($P(q) \sim q^{-1}$) and a Gaussian chain ($P(q) \sim q^{-2}$, see Fig. 6). An increase in M increases R_g , as discussed above, and as a consequence the region at which $P(q) \sim q^{-1.5}$ expands to smaller q -values. The absence of other scattering features suggests that nanogel particles of small mesh size do not exhibit particle-like characteristics.

We find a different type of behavior for nanogel particles having M fixed and increasing the mesh size of the nanogel particle. At intermediate length scales, $\pi/(2M) \lesssim q\sigma \lesssim \pi/M$, a power-law regime emerges that is distinct from the power-law behavior of the linear chains. At these length scales, $P(q)$ reflects the conformation of multiple chains forming an empty compartment in the nanogel structure. This feature is absent in $P(q)$ profiles of smaller in size nanogel particles, suggesting a 'critical' threshold for this type of structures to be identified by scattering experiments. The scaling exponent, μ , in this regime decreases towards zero (an exponent of zero corresponds to a perfect plateau) with increasing the mesh size and for nanogel particles having $M = 15$ as $\mu \sim N_b^{-1.28}$, see inset of Fig. 7.

At length scales larger than R_g , we find a sharp increase in $P(q)$, followed by $P(q)$ eventually reaching a plateau, at which the size of the nanogel particle that probing becomes much smaller in comparison to length scales associated with the scattering. How-

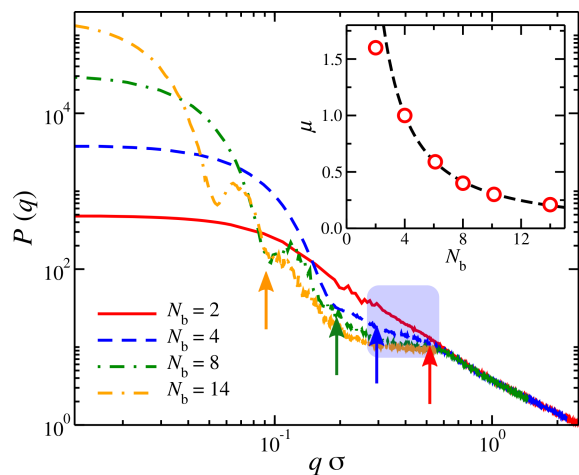


FIG. 7. The form factor $P(q)$ of ideal nanogel particles having $f = 4$ and $M = 15$ with increasing the mesh size, N_b . The arrows indicate the average R_g of the nanogel particles. The light blue highlighted region outlines the emerging power-law intermediate length scales. Inset: the exponent μ characterising the emerging power-law at intermediate length scales in $P(q)$ for nanogel particles having $f = 4$ and $M = 15$ as a function of N_b . The dashed line is a power-law $\mu \sim N_b^{-1.28}$ as a guide for the eye.

ever, nanogel particles having a large enough mesh size $N_b \gtrsim 5$ start to exhibit a scattering peak in $P(q)$ at length scales close to $q\sigma \sim R_g$. The location of this peak scales as $q_{\text{peak}}\sigma \sim M_w^{0.56}$, which is consistent with the mass scaling behavior found for R_g . We also find that $R_g q_{\text{peak}} \approx 1.35$, suggesting that if this ratio is determined for a particular structure then experimentalists could extract the particle's R_g from scattering.

An increase in M enhances the polymer-like characteristics, resulting in less sharp boundaries of the gel particle with the solution and thus, the peak observed in the scattering profiles should become diminished. We quantify this effect by noting that the height of the pre-peak and the height of the first minimum in $P(q)$ as q increases follow a power-law behavior, $P(q_{\text{peak}}) \sim M_w^{-1.7}$ and $P(q_{\text{min}}) \sim M_w^{-1.9}$ (Fig. 8), respectively. This means that as M increases then the difference in height between the first minimum and the peak normalized by the height of the plateau as $q \rightarrow 0$ becomes smaller, i.e., $[P(q_{\text{peak}}) - P(q_{\text{min}})]/P(q \rightarrow 0) \rightarrow 0$ as M increases, see inset of Fig. 8. We also note that the scaling exponent characterizing the nanogel particle at intermediate length scales remains independent of M , provided $M > 10$. For $M = 5$ the chains are not long enough to explore more efficiently the configurational space.

C. ‘Fuzzy sphere’ model and an extension

One of the most widely used descriptions of the nanogels/microgel ‘particles’ is the ‘fuzzy sphere’ model, in which the particles are described by a dense homoge-

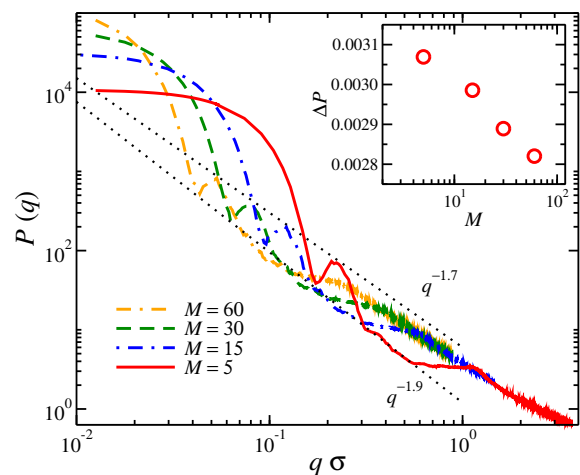


FIG. 8. The form factor $P(q)$ of nanogel particles having a mesh size of $N_b = 8$ and degree of branching $f = 4$. Results of nanogel particles having chain lengths, M , are also presented. The black dotted lines are power-laws with an exponents of -1.9 and -1.7 are a guide for the eye. Inset: Difference between the height of the first peak and the height of the first minimum normalized by the plateau in $P(q)$ at infinite length scales, $\Delta P = [P(q_{\text{peak}}) - P(q_{\text{min}})]/P(q \rightarrow 0)$, as a function of chain length, M .

neous core and an outer loose corona.³⁶ The form factor expression based on the ‘fuzzy sphere’ model is given by,

$$P_f(q, R, \sigma_s)/P_f(q \rightarrow 0, R, \sigma_s) = \left\{ \frac{3 [\sin(qR) - qR \cos(qR)]}{(qR)^3} \exp \left[-\frac{(q\sigma_s)^2}{2} \right] \right\}^2, \quad (4)$$

where R is the size of the particle, σ_s is the smearing parameter corresponding to about half the thickness of the fuzzy shell. A Lorentzian function is also incorporated in the fits to account for the network polymer fluctuations,

$$L(q) = \frac{I(0)}{1 + (\xi q)^2} \quad (5)$$

where ξ is the average correlation length of the nanogel particle’s network, and the amplitude of the long wavelength contribution of the network fluctuations to the intensity $I(0)$. Despite the simple description of the scattering profile by the ‘fuzzy sphere’ model, it has well reproduced the scattering profile of microgels that lack an ordered internal structure, e.g., random crosslinking and entangled chains.^{15,16,36}

A comparison between the fuzzy sphere model and the scattering profiles obtained by our simulation model reveals that the fuzzy sphere model does a satisfactory job in describing $P(q)$ at length scales larger than the nanogel particle size and around the primary peak, see Fig. 9. However, this oversimplified model fails to describe the behavior of $P(q)$ at length scales smaller than $2\pi/q_{\text{peak}}$. In other words, this model fails to describe the

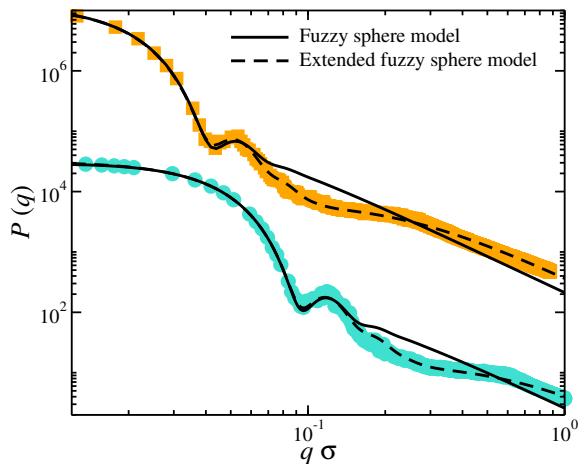


FIG. 9. Form factor, $P(q)$, of nanogel particles having a mesh size $N_b = 8$, degree of branching $f = 4$, and chain length $M = 15$ (circles) and $M = 60$ (squares); the latter is scaled by a factor of 100 for clarity. The lines are fits based on the ‘fuzzy sphere’ and ‘extended fuzzy sphere’ models.

internal structure of the nanogel particle, evidenced by the emergence of the power-law at intermediate length scales as we discussed above, Fig. 7. This limitation is not surprising given the highly coarse-grained nature of this popular model.

To improve upon the ‘fuzzy sphere’ model, we note that an additional term is required to capture the internal structure of the nanogel particle, which resembles a smaller version of the nanogel particle. Based on this observation, we propose the following expression for the fitting of the form factors in our model,

$$P(q)/P(q \rightarrow 0) = P_f(q, R_1, \sigma_{s,1}) + sP_f(q, R_2, \sigma_{s,2}) + L(q) \quad (6)$$

where s is a fit parameter. The first term of this ‘extended fuzzy sphere’ model describes the nanogel particle as a whole having an effective size of $R_1 \approx R_g$. The second term describes the inner structure of the nanogel particle where a second length scale R_2 corresponds to a smaller length scale typically on the order of the size of the repeating structural unit of the nanogel, i.e., star polymer, or smaller. Even though this expression is a highly coarse-grained model of the nanogel particle, it provides a considerably improved description of the nanogel particle’s internal structure, Fig. 9, because it addresses the existence of the internal nanogel structure.

D. Ideal nanogel particles and gels

Now that we have an understanding of the structure of ideal nanogel particles, we briefly discuss them with the structure of ideal macro-gels. It has been reported in the literature that tetra-PEG gels exhibit a near-ideal polymer network topology, i.e., they contain only a small number of pendant chains, trapped entangle-

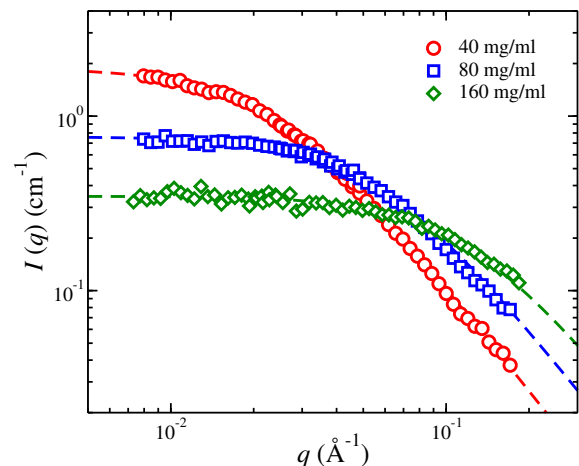


FIG. 10. Small angle neutron scattering (SANS) profiles of tetra-poly(ethylene glycol) (PEG) gels at three different concentrations. The gels were made of 10 kDa precursor chains at (40, 80, and 160) mg/ml concentrations. The dashed lines are fits with a Lorentzian function, see Eq. 5. The data are reproduced from F. Horkay, K. Nishi, and M. Shibayama, J. Chem. Phys. 146, 164905 (2017) with the permission of the AIP Publishing.

ments, and elastically ineffective loops, and the elastic response of tetra-PEG gels is well described by the phantom network model. SANS measurements made on tetra-PEG gels showed that the shape of the SANS profiles resembled that of polymer solutions and could be described by the Lorentzian function, see Fig. 10. These findings were interpreted as providing evidence for the absence of network non-uniformities.⁶⁷ This means that as the polymer network becomes much larger than the size of the polymer chains, then the contribution of these non-uniformities start to diminish.

IV. CONCLUSIONS

In summary, we studied the conformational properties of ideal nanogel particles in athermal solutions using molecular dynamics simulations. In particular, we calculated the mass scaling exponents of the radius of gyration and the hydrodynamic radius, as well as, the intrinsic viscosity with the variation of the degree of branching, the length of the chains between the branched points, and the size of the mesh as a whole. We find competing trends between the molecular characteristics, where an increase in mesh size or degree of branching results in the emergence of particle-like characteristics while an increase in the chain length enhances the polymer-like characteristics. This crossover between these two limiting behaviors is also apparent in the calculation of the form factor, $P(q)$, for these structures. Specifically, a primary scattering peak emerges, characterizing the overall nanogel particle size. Moreover, a distinct power-law regime emerges in $P(q)$ at length

scales larger than the chain size but smaller than the R_g of the nanogel particle and the scaling exponent for this power-law regime goes to zero as the mesh size increases. The ‘fuzzy sphere’ model does not capture the latter feature, and we propose an extension of this popular model to address this shortcoming. Overall, we find that the structural features that characterize these structures become more pronounced when the choice of molecular parameters leads to the localization of the branching segments within the nanogel particle, having an ideal network structure. Overall, we find that the character of the nanogel is sensitive to the number of branched points in its structure, where nearly all particle-like characteristics have emerged at $N_b \gtrsim 6$. On the other hand, the polymer chain length enhances the polymer character of the nanogel particle, but at a slower pace compared to N_b . In subsequent work, we will study nanogel particles where there are many broken bonds since this type of network is characteristic of many real nanogel particles and macroscopic networks. Unsurprisingly, such networks have a much more open, fractal structure and the mass scaling of this type of nanogel particle is altered in comparison to the ‘closed’ nanogel particles studied in the present work which are free of such bonding ‘defects’.

V. ACKNOWLEDGEMENTS

This research was partially supported by the Intramural Research Program of the NICHD, NIH.

VI. DATA AVAILABILITY

The data that support the findings of this study are available from the corresponding author upon reasonable request.

- ¹F. Horkay and P. J. Basser, *Sci. Rep.* **10**, 1 (2020).
- ²B. Xu, *Langmuir* **25**, 8375 (2009).
- ³E. Carletti, A. Motta, and C. Migliaresi, in *Scaffolds for tissue engineering and 3D cell culture* (2011), pp. 17–39.
- ⁴K. R. Hixon, T. Lu, and S. A. Sell, *Acta biomaterialia* **62**, 29 (2017).
- ⁵S. Mantha, S. Pillai, P. Khayambashi, A. Upadhyay, Y. Zhang, O. Tao, H. M. Pham, and S. D. Tran, *Materials* **12**, 3323 (2019).
- ⁶L. Fiorillo and G. L. Romano, *Gels* **6**, 48 (2020).
- ⁷R. M. Martinez, C. Rosado, M. V. R. Velasco, S. C. S. Lannes, and A. R. Baby, *Int. J. Cosmet. Sci.* **41**, 109 (2019).
- ⁸S. Mitura, A. Sionkowska, and A. Jaiswal, *J. Mater. Sci. Mater. Med.* **31**, 1 (2020).
- ⁹P. J. Flory, *Principles of Polymer Chemistry* (Cornell University Press, Ithaca, 1953).
- ¹⁰M. Rubinstein and R. H. Colby, *Polymer Physics* (Oxford University Press, Oxford, 2003).
- ¹¹D. M. Eckmann, R. J. Composto, A. Tsourkas, and V. R. Muzykantov, *J. Mater. Chem. B* **2**, 8085 (2014).
- ¹²J. Li and D. J. Mooney, *Nat. Rev. Mater.* **1**, 1 (2016).
- ¹³W. Yu, R. Liu, Y. Zhou, and H. Gao, *ACS Cent. Sci.* **6**, 100 (2020).
- ¹⁴C. G. Lopez and W. Richtering, *Soft Matter* **13**, 8271 (2017).
- ¹⁵N. Gnan, L. Rovigatti, M. Bergman, and E. Zaccarelli, *Macromolecules* **50**, 8777 (2017).
- ¹⁶A. J. Moreno and F. L. Verso, *Soft Matter* **14**, 7083 (2018).
- ¹⁷A. Martín-Molina and M. Quesada-Pérez, *J. Mol. Liq.* **280**, 374 (2019).
- ¹⁸E. S. Minina, P. A. Sánchez, C. N. Likos, and S. S. Kantorovich, *J. Mol. Liq.* **289**, 111066 (2019).
- ¹⁹M. Shibayama, T. Tanaka, and C. C. Han, *J. Chem. Phys.* **97**, 6842 (1992).
- ²⁰F. Horkay, G. B. McKenna, P. Deschamps, and E. Geissler, *Macromolecules* **33**, 5215 (2000).
- ²¹F. Horkay and B. Hammouda, *Colloid Polym. Sci.* **286**, 611 (2008).
- ²²T. Matsunaga, T. Sakai, Y. Akagi, U. I. Chung, and M. Shibayama, *Macromolecules* **42**, 1344 (2009).
- ²³P. J. Flory, *Proc. R. Soc. London A* **351**, 351 (1976).
- ²⁴B. E. Eichinger, *Macromolecules* **5**, 496 (1972).
- ²⁵B. E. Eichinger and J. E. Martin, *J. Chem. Phys.* **69**, 4595 (1978).
- ²⁶B. E. Eichinger, *J. Chem. Phys.* **75**, 1964 (1981).
- ²⁷G. Ronca and G. Allegra, *J. Chem. Phys.* **63**, 4104 (1975).
- ²⁸G. Ronca and G. Allegra, *J. Chem. Phys.* **63**, 4990 (1975).
- ²⁹S. F. Edwards and T. A. Vilgis, *Rep. Prog. Phys.* **51**, 243 (1988).
- ³⁰G. S. Grest, K. Kremer, and E. R. Duering, *Physica A: Statistical Mechanics and Its Applications* **194**, 330 (1993).
- ³¹F. A. Escobedo and J. J. de Pablo, *Phys. Rep.* **318**, 85 (1999).
- ³²T. Matsunaga, T. Sakai, Y. Akagi, U. I. Chung, and M. Shibayama, *Macromolecules* **42**, 6245 (2009).
- ³³T. Sakai, *Polymer Journal* **46**, 517 (2014).
- ³⁴M. Shibayama, X. Li, and T. Sakai, *Colloid Polym. Sci.* **297**, 1 (2019).
- ³⁵X. Li, S. Nakagawa, Y. Tsuji, N. Watanabe, and M. Shibayama, *Sci. Adv.* **5**, eaax8647 (2019).
- ³⁶M. Stieger, J. S. Pedersen, and P. Lindner, *J. Chem. Phys.* **120**, 6197 (2004).
- ³⁷J. B. Hubbard and J. F. Douglas, *Phys. Rev. E* **47**, 2983 (1993).
- ³⁸M. L. Mansfield, J. F. Douglas, and E. J. Garboczi, *Phys. Rev. E* **64**, 061401 (2001).
- ³⁹D. Juba, D. J. Audus, M. Mascagni, J. F. Douglas, and W. Keyrouz, *Journal of Research of National Institute of Standards and Technology* **122**, doi:10.6028/jres.122.020 (2017).
- ⁴⁰M. L. Mansfield, A. Tsortos, and J. F. Douglas, *J. Chem. Phys.* **143**, 124903 (2015).
- ⁴¹E. H. Kang, M. L. Mansfield, and J. F. Douglas, *Phys. Rev. E* **69**, 031918 (2004).
- ⁴²J. F. Douglas and E. J. Garboczi, *Adv. Chem. Phys.* **91**, 85 (1995).
- ⁴³P. J. Flory, *Statistical Mechanics of Chain Molecules* (Interscience, New York, 1969).
- ⁴⁴T. C. Lubensky and J. Isaacson, *Phys. Rev. A* **20**, 2130 (1979).
- ⁴⁵B. Li, N. Madras, and A. D. Sokal, *J. Stat. Phys.* **80**, 661 (1995).
- ⁴⁶M. Wittkop, S. Kreitmeier, D., and Göritz, *J. Chem. Phys.* **104**, 3373 (1996).
- ⁴⁷K. F. Freed, *J. Chem. Phys.* **79**, 6357 (1983).
- ⁴⁸J. A. M. Smit, J. A. P. P. Van Dijk, M. G. Mennen, and M. Daoud, *J. Chem. Phys.* **25**, 3585 (1992).
- ⁴⁹E. Bouchaud, M. Delsanti, M. Adam, M. Daoud, and D. Durand, *J. Phys. France* **47**, 1273 (1986).
- ⁵⁰J. F. Douglas, *Phys. Rev. E* **54**, 2677 (1996), The scaling exponent ν for polymer without excluded volume is $\nu = 1/4$ and it is not equivalent to branched polymers at their θ -point or having screened excluded volume interactions where $\nu \approx 2/5$. “Percolation clusters” are branched polymers with screened excluded volume interactions.
- ⁵¹W. Burchard, *Adv. Polym. Sci.* **143**, 113 (1999).
- ⁵²A. Chremos and J. F. Douglas, *J. Chem. Phys.* **149**, 044904 (2018).
- ⁵³B. H. Zimm and W. H. Stockmayer, *J. Chem. Phys.* **17**, 1301 (1949).
- ⁵⁴W. H. Stockmayer and M. Fixman, *Ann. N. Y. Acad. Sci.* **12**, 334 (1953).

- ⁵⁵J. F. Douglas and K. F. Freed, *Macromolecules* **27**, 6088 (2014).
- ⁵⁶M. L. Mansfield and J. F. Douglas, *Phys. Rev. E* **78**, 046712 (2008).
- ⁵⁷D. Audus, A. M. Hassan, E. J. Garboczi, and J. F. Douglas, *Soft Matter* **11**, 3360 (2015).
- ⁵⁸M. L. Huggins, *J. Appl. Phys.* **10**, 700 (1939).
- ⁵⁹M. Doi and S. F. Edwards, *The Theory of Polymer Dynamics* (Clarendon Press, Oxford, 1994).
- ⁶⁰K. Ito, Y. Tomi, and S. Kawaguchi, *Macromolecules* **25**, 1534 (1992).
- ⁶¹L. J. Fetters, N. Hadjichristidis, J. S. Lindner, and J. W. Mays, *J. Phys. Chem. Ref. Data* **23**, 619 (1994).
- ⁶²Y. Lu, L. An, and Z.-G. Wang, *Macromolecules* **46**, 5731 (2013).
- ⁶³M. A. Lauffer, *J. Biol. Chem.* **126**, 443 (1938).
- ⁶⁴J. Masuelli, *Polymer and Biopolymer Phys. Chem.* **2**, 37 (2014).
- ⁶⁵A. Einstein, *Ann. Phys.* **19**, 289 (1906).
- ⁶⁶R. K. Mallavajula, D. L. Koch, and L. A. Archer, *Phys. Rev. E* **88**, 052302 (2013).
- ⁶⁷F. Horkay, K. Nishi, and M. Shibayama, *J. Chem. Phys.* **146**, 164905 (2017).